

Change in fayalites with ultraviolet rays and water

KOMORI, Nobuo^{1*}

¹Kamata junior high school

I reported a change in quality of the fayalite from Hachijojima with ultraviolet rays and the water in this meeting two years ago. I did similar experiment with fayalite from Kawamata-machi, Fukushima afterwards.

I purchased these Fayalites from two companies (company A and company B).

These Fayalites were done the ultrasonic cleaning with tap water and distilled water.

The fayalite of company A has weak degree of the weathering in the outdoors.

The fayalite of company B has more intence degree of the weathering in the outdoors than company A. I decided that the fayalite of company A is called sample A and tha fayalite of company B is called sample B. I carried out following experiment using sample A and sample B.

One of sample B which weight is about 2g, are put in the test tube filled with distilled water. The test tube is irradiated with ultraviolet rays with their peak wave length of 254 nm. Another experiment was done as a comparison under the same condition but without ultraviolet. The tubes were irradiated with ultraviolet rays for three months. The illuminance of ultraviolet rays is 40w/m²when the experiments were first strated.

As a result of this experiment, a lot of brown powder was generated in the test tube that was irradiated with ultraviolet rays. It was estimated by XRD analysis that the brown powder might include Fe₂O₃, FeO (OH), MnO₂.

However, the tube without ultraviolet rays irradiation generated no powder. And I did the same experiment using sample A. As a result no brown powder was generated in the test tube that was irradiated with ultraviolet rays and was not irradiated too.

About these result I estimated as follows.

Because the sample B had much quantity of iron ion in the water and the oxidation of iron ion was promoted by ultraviolet rays, so a lot of powder of the iron oxide was produced in water. Because the sample A had very little iron ion in water,so iron oxide hardly occurs.

Keywords: ultraviolet rays, water, fayalite, iron oxide, maghemite, change

Carbon dissolution mechanism in forsterite

MITANI, Saki^{1*}; KYONO, Atsushi¹

¹Graduate School of Life and Environmental Sciences, University of Tsukuba

Introduction

Silicates are major and important minerals that constitute the Earth's crust and mantle. An enormous amount of carbon is also contained in the Earth's interior. Shcheka et al. (2006) studied about carbon solubility in mantle minerals by high temperature and high pressure experiments, and indicated that carbon solubility increases as a function of pressure to a maximum of ~12 ppm by weight in olivine at 11 GPa. In this case, carbon substitutes as C^{4+} for Si^{4+} and occupies SiO_4 tetrahedra as CO_4 tetrahedra. Sen et al. (2013) suggested that significant substitution of C^{2-} for O^{2-} could occur in geological silicate melts/glasses at moderate pressure and high temperature and might be thermodynamically far more accessible than C^{4+} for Si^{4+} substitution. Thus, it has not been perfectly obvious whether carbon substitutes for Si^{4+} and create CO_4 tetrahedra or substitutes for O^{2-} partially and create $Si(O,C)_4/SiC_4$ tetrahedra.

In this study, we determined the carbon dissolution mechanism in forsterite, which is the major minerals in the upper mantle.

Experimental method

Natural forsterite (San Carlos, California, USA) was used in carbon solubility experiments. Forsterite was mixed with either graphite as a crystalline solid or activated carbon as an amorphous form to be homogenized powder. Then, they were heated for 1000 °C, 2 days under ambient pressure. After that, the X-ray powder diffraction study was performed to analyze the change of lattice parameters of the reaction products. The FT-IR study was performed to indicate whether carbon dissolved in SiO_4 tetrahedra. The EPMA analysis was for quantitative analysis of carbon in the reaction products. Moreover, assumption of the reaction product structures was done by the first-principle calculation.

Result and discussion

The X-ray powder diffraction study showed that as increasing the carbon content, the lattice parameters were isotopically contracted. The FT-IR study showed that a C-O bond would be partially formed. Moreover, the EPMA analysis revealed that a small amount of carbon was dissolved in the forsterite with a negative correlation between Si and C. All of the experimental results obtained so far suggested that carbon was able to dissolve in the SiO_4 tetrahedra in forsterite as C^{4+} . The first-principle calculation supported the observed results and the proposed substitution model in the study.

However, the quantity of carbon dissolution in forsterite is low, so we have to repeat verification experiments carefully and lead the conclusion.

Keywords: silicate mineral, carbon dissolution, forsterite

Viscosity of KAlSi_3O_8 melt under high pressure

SUZUKI, Akio^{1*}

¹Tohoku University

Viscosity is a fundamental property controlling the transportation of magma in the planetary interiors. In this study, we measured the viscosity of KAlSi_3O_8 composition of melt under high pressure. The viscosity was measured by the falling sphere method using an X-ray radiography system. Experiments were performed at the NE7A station of the PF-AR synchrotron radiation facility in KEK, Tsukuba, Japan. High pressure was generated using a Kawai-type apparatus driven by a DIA-type guide block in the MAX-III press. A powder of natural sanidine (KAlSi_3O_8) was loaded with a platinum sphere in a molybdenum container. Powder X-ray diffraction data were obtained by energy-dispersive method using a pure Ge solid state detector. Pressures were determined by using an equation of state of MgO. The results show that the viscosity of KAlSi_3O_8 melt decreased with increasing pressure up to 6 GPa.

Keywords: magma, viscosity, high pressure, mantle, synchrotron radiation

Elastic constants of single-crystal quartz and their temperature dependence studied via sphere-resonance method

SEMA, Fumie^{1*} ; WATANABE, Tohru¹

¹Graduate School of Science and Engineering, University of Toyama

Single-crystal elastic constants of rock-forming minerals and their temperature dependence are critical for interpreting observed seismic velocities. A good interpretation requires a thorough understanding of elastic properties of major constituent minerals. Compared with mantle minerals such as olivine, to which a lot of work have been done, elastic properties of crustal minerals have been poorly constrained. Quartz is one of the most abundant minerals in the crust. We have studied elastic constants of single-crystal quartz and their temperature dependence by the sphere-resonance method.

A sphere sample ($D=5.826(1)$ mm) was made from a synthetic quartz single-crystal by the two-pipe method. Resonant frequencies were measured with ultrasonic transducers (Panametrics, V156RM), a lock-in-amplifier (SRS, SR844) and a function generator (Tektronix, AFG320). Measurements were made at frequencies from 400 kHz to 1.2 MHz with different specimen-holding forces. Extrapolating to the specimen-holding force of zero, we obtained frequencies of "free" oscillation. The sample and transducers were placed in a temperature-controlled container. The temperature was changed from 0 to 40°C. Elastic constants were determined by comparing measured and calculated resonant frequencies. The xyz algorithm (Visscher et al., 1991) was employed to calculate resonant frequencies of the sphere sample. Preliminary analysis has shown that C_{11} , C_{33} , C_{44} , C_{12} , C_{13} and C_{14} at room temperature (19.4°C) are 87.224, 105.47, 58.328, 6.885, 11.914, 18.116 (GPa), respectively. The temperature dependence of elastic constants will also be presented in this poster.

Keywords: elastic constants, resonance method, temperature dependence, quartz

A kinetical study of proton dynamics of brucite and portlandite

MASUDA, Manami¹ ; NAGAI, Takaya^{2*} ; KAWANO, Jun²

¹School of Science, Hokkaido University, ²Faculty of Science, Hokkaido University Graduate

Brucite is $Mg(OH)_2$ compound and the crystal structure of brucite is recognized as a prototype of hydrous layered minerals with complicated structures. Various physical and chemical properties of some minerals with the brucite structure such as brucite itself and portlandite, $Ca(OH)_2$ have been investigated. It is especially interesting to understand proton dynamics in hydrous minerals, because the proton diffusion should be closely related to mechanism and kinetics of plastic deformation, hydration, dehydration and so on. Nevertheless, proton diffusion studies on brucite structured minerals have been surprisingly scarce. Recently Noguchi and Shinoda (2010) conducted H-D exchange diffusion experiments on portlandite and Guo et al.(2013) performed proton diffusion experiments on brucite at high pressure. However, it is difficult to understand mechanism of proton diffusion of brucite structured minerals systematically, because their experimental conditions such as pressure and temperature are different. In this study, we performed deuterated experiments for brucite, hydrated experiments for deuterated brucite and deuterated experiments for portlandite at several temperatures and at an atmospheric pressure.

All sample powders were prepared by hydrothermal synthesis and checked the qualities by X-ray diffraction, infrared absorption spectroscopy and SEM. The H-D exchange experiments at several temperatures were performed with a vertical tube furnace in which bubbling dried N_2 gas through D_2O (or H_2O) was introduced. A crucible filled with the sample powder was hung in the middle of the tube furnace. A small amount of the sample powder was picked out at appropriate time intervals and IR measurements for it were performed to know time variation of the molar ratio of D to H.

The diffusion rate depends on temperature and is faster at higher temperature. The diffusion rate also depends on the molar ratio of D to H. Rate control process of proton diffusion in brucite structured minerals will be discussed from diffusion coefficients, activation energies and frequency factors determined.

Keywords: Proton dynamics, H-D exchange, brucite, portlandite, kinetics

Application of the Raman carbonaceous material thermometer to chondrites

HOMMA, Yoshitaka^{1*}; KOUKETSU, Yui¹; KAGI, Hiroyuki¹; MIKOUCHI, Takashi¹; YABUTA, Hikaru²

¹Graduate School of Science, The University of Tokyo, ²Graduate School of Science, Osaka University

Introduction

Structure of carbonaceous material (CM) reflects the experience of thermal metamorphism which occurred on their parent bodies. Therefore, various applications of CM to geothermometer on both terrestrial metasediments and primitive chondrites have been reported so far. Raman spectroscopy is a promising method to investigate the structure of CM, because of the in-situ, non-destructive analysis. Raman spectra of CM have characteristic bands at around 1600cm^{-1} (G-band) and 1355cm^{-1} (D1-band). Recently, detailed analysis on Raman spectra of CM using four or five peaks on terrestrial metasediments extended the applicable range of thermometer to $150\sim 650\text{ }^{\circ}\text{C}$ (Kouketsu et al., 2014). On the other hand, only two peaks are applied in the regression analysis on Raman spectra of CM in meteorites at present. In this research, we try to improve the Raman thermometer on CM in meteorite by applying the detailed peak fitting method.

Samples and Methods

In this research, 20 samples were chosen from carbonaceous chondrites, ordinary chondrites and R chondrites. Raman spectra were obtained on CM in 14 bulk meteorites, thin section of five samples and insoluble organic matter (IOM) extracted from one sample. Laser power at the sample surface was controlled in the range of $1\sim 2.5\text{ mW}$, and acquisition time was $10\sim 30\text{ s}$. For most of the samples, at least 30 data sets were acquired. After removing the background by a linear baseline, the obtained spectra were fitted by four pseudo-Voigt functions.

Results and Discussion

Four-peak spectral fitting (using G_L , D1, D3 and D4-band) was performed on each sample. The result suggested that there is a correlation between the full width at half maximum (FWHM) of D1-band and peak metamorphic temperatures (PMT). A calibration curve was obtained by using seven samples whose metamorphic temperature were already estimated to be $120\sim 550\text{ }^{\circ}\text{C}$ in the previous study (Huss et al., 2006). The derived relationship between the FWHM of D1-band (Γ_{D1}) and PMT is represented by a liner function.

To verify whether the obtained thermometer is applicable to other chondrites, we observed the relationship between Γ_{D1} and other parameters. The relationship between intensity ratio I_{D1}/I_{GL} and Γ_{D1} showed that the value of Γ_{D1} has the lowest limit. This phenomenon was also identified in Kouketsu et al. (2014). From the obtained results, the upper limit of the thermometer was found to be ($550\text{ }^{\circ}\text{C}$).

Conclusion

This study revealed that Raman thermometer on CM is applicable to estimate the metamorphic temperature of primitive chondrites by using the FWHM of the D1-band. The relational is expressed by a linear function and the applicable temperature range is $200\text{ to }550\text{ }^{\circ}\text{C}$. There is a possibility to apply this thermometer to the low metamorphic region under $200\text{ }^{\circ}\text{C}$ by increasing assay samples, although there is still room to optimize the fitting conditions.

Keywords: chondrites, carbonaceous material, Raman spectroscopy, thermal history

Nature of Si-O bonding via molecular orbital calculation

NORITAKE, Fumiya^{1*} ; KAWAMURA, Katsuyuki¹

¹Okayama University

Understanding the nature of Si-O bonding and Si-O-Si bridging is important for mineralogy, material science and metallurgy. It is well known that the variation of Si-O-Si angle in silicates is caused by difference of composition, temperature and pressure. The change of angle of Si-O-Si bridging affects the strength of Si-O bonding. For instance, the increase of Si-O-Si angle decreases the Si-O bond length in coesite crystal (Gibbs et al. 1977). The decrease of Si-O-Si angle of liquid silicates as a result of compression is reported by various researchers (e.g. Navrotsky et al., 1985 Ohtani et al., 1985, Sakamaki et al., 2012). The decrease of Si-O-Si angle is thought to be the trigger of decrease of viscosity of liquid silicates. (Navrotsky et al., 1985, Noritake et al., 2012). Quantum chemical properties of Si-O-Si bridging is investigated to understand the relationship between Si-O-Si angle, Si-O bond length and its strength (e.g., Newton and Gibbs 1980, Tsuneyuki 1996, Kubicki and Sykes 1993). Newton and Gibbs (1980) reports the pyrosilic acid molecule has energy minimum at Si-O-Si angle of 145 ° using STO-3G basis set (Hehre et al 1969) by Hartree-Fock method. Tsuneyuki (1996) reports that the bending of Si-O-Si is not reproduced using double-zeta function basis set nevertheless the increase of the number of basis function generally increase the reproducibility. However, the nature of Si-O-Si bridgings seems not to be reproduced by increase of basis function using Hartree-Fock method. In this paper, we show the molecular orbital calculation about pyrosilic acid molecule using post-Hartree-Fock method and more precise basis set to understand the nature of Si-O-Si bridging.

Molecular orbital calculations were performed using the GAUSSIAN 09 code. We firstly calculate the optimized structure of disiloxane (Almenningen et al., 1963) by Hartree-Fock (HF), second-order Moller-Plesset perturbation theory (MP2), and two density functional theory (Becke's density functional (Becke, 1988) with three correlation functionals by Lee, Yang and Parr (B3LYP) (Lee et al., 1988), and generalized gradient approximation by Perdew, Burke and Ernzerhof (PBE) (Perdew et al., 1996)) with 6-311G(d,p) split valence double zeta basis set (Raghavachari et al., 1980). The bending of Si-O-Si bridging is not reproduced by HF method as shown in Tsuneyuki (1996). The bending of Si-O-Si bridging is reproduced by use of MP2 and density functional theory with PBE. The optimized angle of Si-O-Si in disiloxane molecule by MP2 is closer to experimental value than that by PBE. Then we apply the MP2 method with 6-311G(d,p) basis set to the calculation of pyrosilic acid, H₆Si₂O₇. NBO analysis (Foster and Weinhold, 1980, Reed et al., 1985; 1988) is used to analyze the electronic state of bonding.

We found the equilibrium geometries for bended two pyrosilic acid molecules (C_{2v} and 60 ° torsion) using Moller-Plesset perturbation theory and with 6-311G(d,p) split valence double zeta basis set. We calculated the energy surface with varying Si-O_{br} length and Si-O-Si angle and found the relationship between Si-O_{br} length and bridging angle. From the energy surface, the stable Si-O bond length decrease with spreading Si-O-Si angle. The bending of Si-O-Si angle in equilibrium geometries can be explained by explained by the balance of Coulombic repulsion between tetrahedra and lone pair electrons of bridging oxygen atom without concerning the contribution of d-p π-bonding. The Si-O bonding strengthen with increasing Si-O-Si angle because of stabilization in energy of Si-O bonding orbital with decreasing the hybridization index λ in sp^λ orbital of bridging oxygen and increase of coulombic interaction between Si and bridging oxygen atom.

Keywords: Molecular orbital calculation, Si-O-Si bridging

Bule cathodoluminescence derived from defecte centers in magnesite

KUSANO, Nobuhiro^{1*} ; NISHIDO, Hirotsugu¹ ; NINAGAWA, Kiyotaka¹

¹Okayama University of Science

Cathodoluminescence (CL) has been widely applied in mineralogical and petrological investigations, especially for carbonates. Although most calcite-type carbonates exhibit red to orange CL activated by divalent Mn ions, blue CL is uncommon in carbonates, but not with bright emission (e.g., Machel et al., 1991). Magnesite occasionally shows red CL emission assigned to an impurity center of divalent Mn ion substituted for an Mg ion as an activator (Medlin 1963, Sommer 1972), but not usually accompanied by blue emission. We have confirmed a significant blue emission in the CL of magnesite from Tennohama, Wakayama, Japan.

Blue luminescent magnesite (BM) occurs as a rhombohedral crystal in hydrothermal veinlets associated with dolomite and quartz. Its single crystal in size of 2-3 mm has been employed for CL measurements, as well as a single crystal of common magnesite (RM) with red CL emission from Brumado, Brazil. Color CL images were obtained using a cold-cathode type Luminoscope with a cooled-CCD camera. CL spectroscopy was made by a SEM-CL system, which is comprised of SEM (JEOL: JSM-5410LV) combined with a grating monochromator (OXFORD: Mono CL2). The CL emitted from the samples was dispersed by a grating monochromator (1200 grooves/mm), and recorded by a photon counting method using a photomultiplier tube. All CL spectra were corrected for total instrumental response, which was determined by use of a calibrated standard lamp.

BM spectrum shows an enhanced broad-band emission with triplet peaks from 300-400 nm in a blue region and a broad-band emission at ~670 nm in a red region, whereas RM has an intense broad band emission at ~670nm previously reported in magnesite samples (e.g., Sommer, 1972) and no emission in a blue region. Blue CL emissions of BM is possibly to be the "background blue" found in the calcite contained almost no activator (Richter and Zinkernagel, 1981), which might be related to an intrinsic defect center. In the case of BM, its emission band in a blue region has triplet peaks with high intensity, but a single broad band with low intensity for calcite.

Therefore, a Gaussian fitting of BM spectrum in an energy unit successfully deconvolutes three emission components at around 2.52 eV (492 nm), 3.28 eV (378 nm) and 3.88 eV (320nm) in a blue region. Kusano et al. (2014) reported a blue CL emission in the calcite with emission components at 2.67eV (464nm) and 3.30eV (376nm), which is the material decomposed from dolomite in the process of skarn mineralization at high temperature. It suggests that the CL derived from defect centers in BM might be attributable to its thermal history during crystal growth.

Keywords: magnesite, cathodoluminescence, blue emission, defect center

Cathodoluminescence characterization of enstatite in meteorites.

OHGO, Syuhei^{1*} ; NISHIDO, Hirotsugu¹ ; NINAGAWA, Kiyotaka¹

¹Okayama University of Science

Enstatite in meteorites occasionally shows various cathodoluminescence (CL) emissions with red, reddish purple and blue, whereas terrestrial enstatite has almost no CL emission. We have confirmed several luminescent enstatite in enstatite chondrite (E-chondrite) and enstatite achondrite (Aubrite). In this study, we have conducted to clarify the luminescence centers of CL emissions in extraterrestrial enstatite compared to the CL of terrestrial enstatite.

The polished thin sections of E-chondrites (Sahara 97096, Sahara 97121, Dar al Gani 734 and Y 86004) and Aubrite (Al Haggounia 001) were used for CL measurements. Color CL images were obtained using a cold-cathode type Luminoscope with a cooled-CCD camera. CL spectroscopy was made by a SEM-CL system, which is comprised of SEM (JEOL: JSM-5410LV) combined with a grating monochromator (OXFORD: Mono CL2). The CL emitted from the samples was dispersed by a grating (1200 grooves/mm), and recorded by a photon counting method using a photomultiplier tube. All CL spectra were corrected for total instrumental response, which was determined using a calibrated standard lamp.

Color CL imaging reveals various types of CL emissions with red, reddish purple and blue in the extraterrestrial enstatite. The CL spectra of these enstatite show a broad emission band at 670 nm in a red region, which is assigned to an impurity center derived from activated divalent Mn ion substituted for Mg, and a broad emission band at around 400 nm in a blue region, which might be related to a defect center possibly assigned to "intrinsic defect center" derived during crystal growth.

CL spectra were converted into energy units for spectral deconvolution using a Gaussian curve fitting, because one Gaussian curve in energy units should correspond to one specific type of emission center (Stevens-Kalceff, 2009). The deconvoluted components can be assigned to the emission centers related to impurity centers of trivalent Cr ion at 1.64 eV and divalent Mn ion at 1.86 eV and two defect centers at 2.71 and 3.18 eV. The emission component at 3.18 eV might be attributed to the defect center of structural distortion by the substitution of Al ion for Si in a tetrahedral site, which is possible to be in the process of crystal growth at high temperature in its parent body (e.g., the rocks hosting Al-rich enstatite formed at depths from 25 km to 130?200 km in the lunar rock; Nazarov et al., 2011). Al contents in blue luminescent enstatite are higher than that in red luminescent one. Blue emission center can be detected in the CL of terrestrial samples.

Keywords: Enstatite, Cathodoluminescence, E-chondrite, Emission center

Self-diffusion of hydrogen in high-pressure ices: Preliminarily results

NOGUCHI, Naoki^{1*} ; OKUCHI, Takuo¹ ; TOMIOKA, Naotaka²

¹Institute for Study of the Earth's Interior, Okayama University, ²Japan Agency for Marine-Earth Science and Technology

High-pressure ices are the primary constituents of mantles of the large icy bodies such as some of Galilean satellites and Edgeworth-Kuiper Belt Objects. Understanding self-diffusion of hydrogen in these high-pressure ices is essential to discuss about mantle dynamics of the large icy bodies because it controls rheology of these ices. In addition, diffusive properties of high-pressure ices are also an interesting topic in the field of high-pressure material science. Shortening of intermolecular distance with increasing pressure induces drastic changes of hydrogen-bonding property such as proton tunneling, proton symmetrization (Benoit et al. 1998), hydrogen sublattice melting (Cavazzoni et al. 1999), and proton hopping transition (Noguchi et al. 2014). Whether these changes of hydrogen bonding affect hydrogen diffusion or not is a major subject in the proton dynamics at high pressure. To elucidate these questions, we have carried out an experiment to determine hydrogen diffusion coefficients of the high-pressure ices using a diamond anvil cell (DAC) and Raman spectroscopy.

The diffusion couples have been prepared from polycrystalline H₂O and D₂O ices prepared within a sample chamber of DAC. The diffusion experiments of these couples were carried out using an electric furnace. Temperatures were set in a range between 400 K and 500 K. After keeping the DAC in the furnace for a few days, Raman mapping measurements of the diffusion couples were carried out at room temperature. Two-dimensional diffusion profiles of deuterium were determined using quantitative curves for deuterium concentration. The quantitative calibration curves were functions as the relative area of Raman band of OH stretching mode to that of OD stretching mode, or Raman shifts of OH and OD stretching modes. Preliminarily results will be reported in our presentation.

Keywords: high-pressure ices, self-diffusion, rheology, Raman spectroscopy

Structure investigation of mordenite induced by molecular sieve using the Rietveld method

SUGANO, Neo^{1*}

¹Life & Env. Sci. Univ. of Tsukuba

[Introduction]

There are a large number of natural and synthesis zeolite minerals that are generally composed of Si/AlO₄ three-dimensionally framework structure. All of them have a porous structure that can adsorb water molecules in their micropores. In addition, zeolite minerals have the highly adsorption and preservation properties generally called molecular sieve that accommodate a variety of cations and molecules in the micropore due to the negative electric charge caused by the substitution of Al₃⁺ for Si₄⁺. The high cation exchange ability has been received great attention in many fields.

Mordenite [(Na₂, Cs, K₂)₄(Al₁₈Si₄₀)O₉₆·28H₂O] (Martucci et al., 2003) is well known for its high selectivity for radioactive Cs and Sr. However, there are only few studies that addressed the crystal structural change of mordenite by Cs⁺-ion exchange molecular sieve. Hence, this study is aimed to clarify the relationship between molecular sieve and structural change of mordenite.

[Experimental Methods]

The structural change of mordenite were investigated by the Rietveld refinement analyses based on the powder X-ray diffraction. measurements; CuK α ($\lambda = 1.54056 \text{ \AA}$), $5^\circ \leq 2\theta \leq 120^\circ$, scanning speed = $4^\circ/\text{min}$, scanning width = 0.02° . Cs-exchanged mordenite were prepared from H-mordenite by ion exchange in CsCl solutions with various Cs concentration (0.010, 0.10, 1.0, 2.0, 4.0, 8.0, 10.0, 30.0g/l) . Cs-exchange experiments were executed by the shaking (32rpm) for 48hrs. The temperatures of solutions were maintained around 20°C.

[Results and Discussion]

The pH value of the solutions was initially 3.44 ± 0.02 , but it was decreased to $2.70-3.09 \pm 0.02$ with addition of mordenite. The decreasing of pH value with the Cs concentration indicated that Cs⁺-ion was substituted for H⁺-ion within the micropore of mordenite structure. Consequently, the lattice parameter of mordenite was isotropically decreased with the Cs⁺-ion concentration. The unit cell volume of mordenite was slightly decreased from 2880 (12) \AA^3 to 2836 (12) \AA^3 (at most 44 (17) \AA^3).

The molecular sieve of mordenite was characterized by the contraction of 12-membered ring channel (12MRc) and 8-membered ring channel (8MRc) where the Cs⁺-ion can be accommodated within the mordenite structure. The 12MRc with the largest pore size was appropriately contracted with the Cs content due to the electrostatic attraction between Cs⁺-ion and framework atoms. The contraction of 12MRc (at most 0.31(8) \AA) especially acted toward the direction of b-axis. The high absorption efficiency of the molecular sieve is caused by the site preference of Cs⁺-ion into the 12MRc. The 8MRc with the smaller pore size than the 12MRc directly connected with the 12MRc. It behaves in the opposite way to the 12MRc. The 8MRc is strongly affected with the structural modification of 12MRc. Since the Cs⁺-ion are hardly incorporated into the 8MRc, the site occupancy of Cs⁺-ion in the 8MRc is always lower than that in 12MRc, which leads to the small contraction values of 8MRc.

Keywords: Mordenite, Molecular sieve, Rietveld refinement

In situ high pressure IR spectroscopic observations on the upper mantle anhydrous minerals using diamond anvil cell

SAKURAI, Moe^{1*} ; TSUJINO, Noriyoshi² ; TATENO, Shigehiko³ ; SUZUKI, Toshihiro¹ ; YOSHINO, Takashi² ; KAWAMURA, Katsuyuki⁴ ; TAKAHASHI, Eiichi¹

¹Earth and Planet. Sci., Tokyo Tech, ²ISEI, Okayama Univ., ³ELSI, Tokyo Tech., ⁴Environmental and Life Sci., Okayama Univ.

Most nominally anhydrous minerals (NAMs) in the Earth's upper mantle can contain small amounts of hydrogen (i.e. "water"), structurally bond as hydroxyl. Structurally bounded water causes important influences on many physical properties of mantle rocks. The influence seems to be controlled by hydrogen atoms positions in crystal structure. In most of previous researches, hydrogen atoms positions have been estimated by comparison between the theoretically calculated IR spectra and the experimental results, which obtained at ambient pressure [1, 2]. Therefore, the influence of pressure on hydrogen atom positions has not been identified yet. However, the physical properties relating to hydrogen atom (electric conductivity, viscosity and more), have been measured at high pressure conditions. Thus it is important to clarify the influence of pressure on hydrogen atoms positions.

To observe the influence of pressure on IR spectra, high-pressure experiments have been conducted at pressures of 0.4 – 9.0 GPa at room temperature. The experiments were performed with diamond anvil cell by using natural olivine (Ol) and synthetic forsterite (Fo) as starting materials. The pressure medium was KBr powder or fluorinert. Pressure was determined by ruby fluorescence method [3]. The IR spectra were obtained with a vacuum type Fourier transform infrared spectrometer (Jasco: FT-IR6100, IRT5000).

Clear OH stretching vibration bands could be observed for samples with water concentration over ~100 wt.ppm. The non-polarized IR spectrum of synthesized Fo showed four bands; two stronger ones at 3610, 3575 cm⁻¹ and two weaker bands at 3550, 3475 cm⁻¹ at ambient pressure. The band at 3475 cm⁻¹ disappeared in the spectrum of randomly oriented Fo at ≥5.6 GPa. The band at 3610 cm⁻¹ shifted to low wavenumber with increasing pressure. After decompression, the spectrum return to the almost same position and intensity before increasing pressure. Thus it indicates that these bands shift is a reversible change.

The polarized to *a*-axis IR spectrum of natural Ol showed three bands; 3610, 3598 and 3575 cm⁻¹ at ambient pressure. The band at 3610 cm⁻¹ shifted to low wavenumber and became weaker with increasing pressure. The band at 3575 cm⁻¹ shifted to high wavenumber, which results is opposite to the band at 3610 cm⁻¹, and also became weaker with increasing pressure. The polarized to *b*-axis IR spectrum of natural Ol showed two bands; 3598 and 3575 cm⁻¹. The band at 3598 cm⁻¹ did not change with increasing pressure. In this experiment, the diamond anvils touched sample directly above 8 GPa, so we could not observe the spectrum after decompression.

[1] Umemoto et al.: *Am. Min.*, 96, 1475-1479, 219 (2011) [2] Sakurai et al.: *J. Comput. Chem. Jpn.* [3] Mao et al.: *J. Appl. Phys.* 49, 3276-3283 (1978)

Keywords: FT-IR, Pressure effect, Nominally anhydrous minerals, Upper mantle, In situ experiment

Study on the stability of the $\text{Al}_{65}\text{Cu}_{20}\text{Fe}_{15}$ icosahedral quasicrystal using Synchrotron X-ray diffraction method

TAKAGI, Sota^{1*}; KYONO, Atsushi²

¹College of Geoscience, School of Life and Environmental Sciences, University of Tsukuba, ²Graduate School of Life and Environmental Sciences, University of Tsukuba

The stability of the $\text{Al}_{65}\text{Cu}_{20}\text{Fe}_{15}$ icosahedral quasicrystal at high pressure and high temperature has been investigated using synchrotron X-ray diffraction method. High pressure *in situ* XRD experiments were performed up to 104 GPa, and high pressure and high temperature *in situ* XRD experiments were performed at the pressure points of 11, 24, 33, 57, 67, 104 GPa up to temperature of about 2500 K. The high pressure experiments revealed that five characteristic XRD peaks of the $\text{Al}_{65}\text{Cu}_{20}\text{Fe}_{15}$ icosahedral quasicrystal remained up to 104 GPa at room temperature, while a new peak appeared at the point of $d = 2.90 \text{ \AA}$ above 89 GPa. The six-dimensional lattice parameter, a_{6D} , was continuously contracted from 12.5 \AA to 11.2 \AA with pressure. The bulk modulus of the $\text{Al}_{65}\text{Cu}_{20}\text{Fe}_{15}$ icosahedral quasicrystal started to change around 70 GPa. This result suggested that the $\text{Al}_{65}\text{Cu}_{20}\text{Fe}_{15}$ icosahedral quasicrystal was transformed to high pressure phase at about 70 GPa. The high pressure and high temperature experiments showed that a different phase (high-temperature phase) occurs as a function of the temperature. The phase boundary between the $\text{Al}_{65}\text{Cu}_{20}\text{Fe}_{15}$ icosahedral quasicrystal and its high temperature phase was risen with pressure, such as 865 K at 11 GPa, 1402 K at 24 GPa, 1758 K at 33 GPa, 1963 K at 57 GPa, 2050 K at 67 GPa, 2080 K at 104 GPa. In a series of the study, the $\text{Al}_{65}\text{Cu}_{20}\text{Fe}_{15}$ icosahedral quasicrystal was melted completely only when it was heated to 2385 K at 11 GPa. From the present study, it was suggested that mineral icosahedrite ($\text{Al}_{63}\text{Cu}_{24}\text{Fe}_{13}$), the first natural-occurring quasicrystal, was formed at pressure range from 5 GPa to 70 GPa, and at temperature range from 1500 K to 2200 K. This study can be a clue to solve the question of where and how the icosahedrite was formed.

Keywords: $\text{Al}_{65}\text{Cu}_{20}\text{Fe}_{15}$ icosahedral quasicrystal, icosahedrite, stability, high pressure and high temperature, XRD

Observation of morphological behavior with heating of volcanic ash by in situ particle image analysis

HAMADA, Hiroyuki^{1*} ; KANATSUKI, Shinichiro² ; HAYAUCHI, Aiko¹ ; SASAKURA, Daisuke¹

¹Malvern Instruments, A division of Spectris Co., Ltd., ²Japan High Tech Co., Ltd.

1. Introduction

An *in-situ* observation to particle morphology under any perturbations is well used to understand physical chemistry behavior of mineral particles. With using by a heating response as a one of perturbation is interesting to investigate to melting and crystallinity of minerals. One of drawback to particle morphology investigation by a manually microscope is a qualitative approach rather than quantitative approach.

Our group has reported particle characterization and classification of a volcanic ash fine particle using by images for the purpose of determining particle size distribution which is based on described in ISO13322. The particles are appropriately dispersed and fixed on an optical microscope implemented an automated real time particle image analysis function on software. This report will be discussed for observation of morphological behavior with heating of volcanic ash by in situ particle image analysis.

2. Material and Method

In this study, the volcanic ash was sampling from Ito flow in Kagoshima. As a statistical particle image analysis, an automated particle image analyzer, Morphologi G3-SE (Malvern Instruments) was used for evaluation of particle size and shape. The observation mode was reflectance mode magnification was 75x in total magnification. The sample was dispersed with SDU (Sample Dispersion Unit) which attached Morphologi G3-SE. Number of measured particles was several hundred and a parameter filter function on software was used based on shape and pixel number of particle image. As a heat stage, Linkam stage TS1500 (Japan Hightech Co., Ltd.) was use for sample heating up to 1500 °C. A sample particle was dispersed on a platinum sample cell by SDU.

3. Result and Discussion

As a result of feasibility study, Fig.1 shows the observed images at 30 °C, 500 °C, 1000 °C, and 1500 °C. No change was observed between 30 °C and 1000 °C. However, the significant change of particle morphology by melting was observed between 1000 °C and 1500 °C. Refer to result of feasibility test, the temperature range from 1000 °C to 1500 °C is appropriate for this investigation.

4. Conclusion

In summarize of this study, it was possible to observe particle morphology change by heating. This report will be more discussed about the application and the capability for more quantitative investigation by particle image analysis.

Keywords: volcanic ash, microscopy, particle image analysis, particle diameter, particle distribution

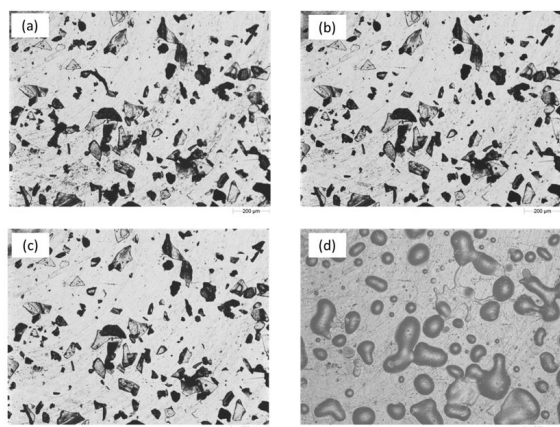


Fig.1 Particle morphology change under heating. (a)30°C (b)500°C (c)1000°C (d)1500°C

Magnetic measurement of H₂O at low-temperature and high-pressure

KONDO, Tadashi^{1*} ; KAKEDA, Takafumi¹ ; TANIGUCHI, Toshifumi¹

¹Graduate School of Science, Osaka University

Water ice is universal material in space and has fifteen polymorphs reported so far. Because of difficulty in detection of subtle structure change corresponding to hydrogen shift, and slow kinetics of low-temperature ice, some phase boundaries at low temperature are still not confirmed experimentally, which is very important information in planetary science. In this study, we tested a possibility of new method for studying structural change of ice using magnetic measurement at low-temperature and high-pressure. H₂O is diamagnetic substance, and the signal intensity of magnetic susceptibility is not detectable if we use a conventional method of magnetic measurement. However, positional ordering of hydrogen atoms should change the spin state of ice. Therefore, we can expect finite change in magnetic susceptibility.

Magnetic measurements were conducted in Superconducting Quantum Interference Device magnetometer (SQUID, MPMS-7, Quantum design). We measured the magnetic moment of ice at temperature below room condition. The measurement was also conducted at high-pressure condition to 0.2GPa to detect phase boundary between phase IX and phase I. Highly purified water with 5 M ohm resistivity or salted waters was used as starting sample in the Teflon capsule with /without a piston cylinder type high pressure cell made of beryllium copper alloy. After many trials of accurate evaluation of magnetic moment of all material surrounding sample as background signal to be subtracted, we measure the signal with water ice in the capsule. The magnetic field applied was 1T. The sample was first cooled to around 100K, then, the temperature elevated to room condition at the rate of 0.25K/s.

Solid-liquid transition of pure water was reproducibly detected with abrupt decrease of magnetic susceptibility. In the case of salt water, magnetic susceptibility decreased gradually with a temperature width as figured by thermodynamics. In the high-pressure run, we found an another jump in the profile of magnetic susceptibility measurement. The condition was close to solid-solid phase boundary proposed. We will report further detail of the experiments as possible detection of phase change in low-temperature water ice.

Keywords: water ice, magnetic measurement, high pressure, phase transition, SQUID